

Exposure Time Change Attack on Image Watermarking Systems

Kaituo Li^{1,*}, Dan Zhang², and De-ren Chen²

¹ College of Software Technology, Zhejiang University, Hangzhou 310027, China
lee.kaituo@gmail.com

² College of Computer Science and Technology, Zhejiang University,
Hangzhou 310027, China
zhangdanny@nbip.net, drc@zju.edu.cn

Abstract. We propose an effective attack based on exposure time change and image fusion, called ETC attack. First, the ETC attack simulates a set of images with different exposure time using the watermarked image. Then it applies an image fusion method to blend the multiple images mentioned above and thus generates a new image similar to the original one. In this paper, we describe the rationale of the attack. To illustrate the effect of the ETC attack, we present the results of the ETC attack against one watermarking scheme Iterative Watermarking Embedding. It can be shown that the ETC attack has an important impact on watermark decoding and detection, while not severely reducing the quality of the image.

1 Introduction

Digital watermarking technology is the process of watermark host analysis, medium pre-processing, embedded information selection and embedding pattern design. It tries to seek an optimum scheme while keeping balance between transparency and robustness. Transparency refers to the imperceptibility of watermark. Robustness means that the inserted watermark is hard to remove. Along with the watermarking technologies, digital watermark attack appears. In fact, the watermark embedding can be regarded as efforts in defense of host image from the watermark attack. The watermark attack aims at breaking the practicality of the watermark and keeping the host work worthwhile at the same time, like removing the watermark or invalidating the extraction algorithm.

In fact there are two main types of attacks: those who attempt to remove the watermark and those who just prevent the detector from detecting them [1]. Attacks in the first category usually try to estimate the original non-watermarked cover-signal, considering the watermark as noise with given statistic. For instance, Maes presented a twin peaks attack to fixed depth image watermarks [2]. The attack is based on histogram analysis. If watermarked images with twin peaks of histogram are observed, we could reconstruct the histogram of the original image and estimate the watermark. Attacks in the second category, such as

* This research is supported partly by the National Basic Research Program of China (973 Program) under Grant No. 2006CB303104.

cropping, horizontal reflection and deletion of lines or columns, try to change the content of watermarked images to make detectors cannot find watermark.

In this article, we propose an attack, called *exposure time change attack* (ETC), which aims at decreasing the cross-correlation score between the original watermark and the decoded watermark. ETC is a new breed of attack against generic image watermarking systems, that is, the ETC attack is not limited to a particular image watermarking algorithm. In order to launch the attack successfully, the adversary does not need to know the details of the watermarking algorithms and the watermarking keys. Also, the ETC attack requires no detectors. Only one copy of watermarked image is needed to break the watermark. In this paper, to illustrate the effect of the ETC attack, we present the results of the ETC attack against one watermarking scheme Iterative Watermark Embedding (IWE). The ETC attack can also be launched for many other watermarking technologies, such as Cox's spread spectrum watermarking [3] and Xia's watermarking [4]. It can be shown that the attack has an important impact on watermark decoding and detection, while not severely reducing the quality of the image. The strategy of an ETC attack contains two steps:

- *Step 1*: simulate a set of images with different exposure time using the watermarked image;
- *Step 2*: apply an image fusion method to blend the multiple images mentioned above.

This paper is organized as follows. The watermarking algorithm IWE is briefly reviewed in Sec. 2. The proposed ETC attack algorithm and the experimental results of the ETC attack against IWE are discussed in detail in Sec. 3 and 4. Discussion is presented in Sec. 5.

2 Reviewing the IWE

In this section, the watermarking scheme IWE presented by [5] is reviewed. The Single Watermarking Embedding (SWE) is introduced at first, since IWE is based on SWE.

2.1 Reviewing the SWE

The sequence that is used to embed a watermark bit sequence comes from the first P percent AC coefficients of the JPEG compressed domain. The sequence is called the host vector. For each of the 8×8 blocks in a JPEG compressed image, the first AC coefficient in zigzag order is extracted and ordered to form the first segment of the vector [5]. Next, the second AC coefficient in zigzag order is extracted and appended to the first segment of the vector and so on, until P percent of the AC coefficients are extracted. The host vector Y is defined as $Y = [y_1, y_2, \dots, y_M]$ with length M . Watermark sequence $W = [w_1, w_2, \dots, w_N]$ is a binary sequence with length N , where $M \gg N$. To embed the N bit watermark into M coefficients, the host vector Y is divided into N sub-vectors

of length $P = \lfloor M/N \rfloor$. One bit watermark is inserted into every sub-vector. SWE uses two keys. The first key $D = [d_1, d_2, \dots, d_N | d_i \in R^+, 1 \leq i \leq N]$ is a set of N pseudo-random positive real numbers. The second key is $K = [k_1, k_2, \dots, k_M]$ with every key k_i being zero-mean Gaussian. Using these two keys, SWE embeds W into Y , and decodes watermark. The watermarked host vector Y is denoted by Y' . Based on above definitions, the basic embedding is shown as follows:

$$Y'_i = Y_i + \alpha_i K_i \tag{1}$$

$$\alpha_i = \begin{cases} \frac{d_i \cdot \text{round}(\langle Y_i, K_i \rangle / d_i) - \langle Y_i, K_i \rangle}{\|K_i\|_2^2}, & \text{for case 1,} \\ \frac{d_i \cdot [\text{round}(\langle Y_i, K_i \rangle / d_i) + 1] - \langle Y_i, K_i \rangle}{\|K_i\|_2^2}, & \text{for case 2,} \\ \frac{d_i \cdot [\text{round}(\langle Y_i, K_i \rangle / d_i) - 1] - \langle Y_i, K_i \rangle}{\|K_i\|_2^2}, & \text{for case 3,} \end{cases} \tag{2}$$

Case 1: $\lfloor \text{round}(\langle Y_i, K_i \rangle / d_i) \rfloor_2 = w_i$

Case 2: $\lfloor \text{round}(\langle Y_i, K_i \rangle / d_i) \rfloor_2 \neq w_i$ and $\langle Y_i, K_i \rangle \geq d_i \cdot \text{round}(\langle X_i, K_i \rangle / d_i)$

Case 3: $\lfloor \text{round}(\langle Y_i, K_i \rangle / d_i) \rfloor_2 \neq w_i$ and $\langle Y_i, K_i \rangle < d_i \cdot \text{round}(\langle X_i, K_i \rangle / d_i)$

The blind watermark decoding and detection is defined as follows:

$$w'_i = \lfloor \text{round}(\langle Y'_i, K_i \rangle) / d_i \rfloor_2 \tag{3}$$

The cross-correlation score s_1 is used to test the watermark is present or not:

$$s_1 = \frac{\sum_{i=1}^N (2 \cdot w_i - 1) \cdot (2 \cdot w'_i - 1)}{\sqrt{\sum_{i=1}^N (2 \cdot w_i - 1)^2 \cdot \sum_{i=1}^N (2 \cdot w'_i - 1)^2}} \tag{4}$$

2.2 Reviewing the IWE

Under JPEG recompression attack, SWE cannot decode and detect the watermark correctly [5]. IWE is proposed to prevent the removal of the watermark in the JPEG recompression attack. Also, SWE is adopted as one part of IWE. Before SWE, Y_i is added to a random noise sub-vector N_i of length P . Each element of the random noise is uniformly distributed in $[-q/2, q/2]$ where q is the JPEG quantization step size (accounting for both the quantization matrix and the scaling factor). Then SWE is performed. After that, a trial JPEG re-quantization and watermark decoding is performed on the watermarked sub-vector. If computed s_1 is below the threshold value or the number of iterations exceeds a pre-defined threshold T , the iteration is forced to terminate. Otherwise, another iteration is carried out. Please refer to Fig. 5.1 in [5] for more details.

2.3 The Robustness of IWE

IWE is tested under StirMark 4.0 attacks [5]. Experiments show that IWE is robust to JPEG compression attacks, small median filtering attacks, watermark

embedding attacks, rotation-and-cropping attacks, rotation-and-scaling attacks, latest small random distortion attacks. IWE is not robust to affine transformation attacks, Gaussian filtering attacks, large noise attacks, rescaling attacks, lines removal attacks, large rotation attacks, large median filtering attacks. But most of the images under attacks in the second category are highly distorted. Thus, IWE is robust to attacks that do not degrade image quality severely.

3 ETC Phase 1: Changing Exposure Time

3.1 Introduction

Exposure time is the duration for which the light sensing element (CCD or film) is exposed to light from the scene. Exposure time is determined by camera shutter speed. The exposure of an image X is defined as [6]:

$$X = Et \tag{5}$$

where E is the irradiance that the light sensing element receives and t is the exposure time. Exposure time can have a dramatic impact on the image pixel values: if the scene luminance is constant, longer exposure time can make the image brighter; shorter exposure time can make the image darker. Varying exposure time can be used to adjust image brightness.

We find that many image watermarking systems can not derive the correct decoded watermark when the watermarked image is exposed differently. This is the main reason why we choose exposure time change as the watermark attack method. In addition, by making some adjustments to the exposure time of the watermarked images, we could simulate the physically-based photorealistic images. That is, we could capture the contents of these simulated images using our cameras. Thus, the resultant images are likely to preserve good image quality and look natural.

3.2 The Relationship between the Image Exposure Time Change and Change of Pixel Value

To illustrate the relationship between the image exposure time change and change of pixel value, we need to know the relationship between the image pixel exposure x and its intensity p . In [7], the relationship between the pixel value p (with a range between 0 and 255 corresponding to 8-bit quantization) and the exposure level x in Jm^{-2} is expressed using the Eq. (6):

$$p = \phi(x) = \frac{255}{1 + e^{-0.75 \cdot \log_{10} x}}, \tag{6}$$

If we change exposure time from t_1 to t_2 and E is constant, the pixel value p_1 in one location turns to p_2 . According to Eq. (5), we get

$$x_1 = Et_1, \tag{7}$$

$$x_2 = Et_2, \quad (8)$$

Thus,

$$p_1 = \phi(x_1) = \frac{255}{1 + e^{-0.75 \cdot \log_{10} x_1}}, \quad (9)$$

$$p_2 = \phi(x_2) = \frac{255}{1 + e^{-0.75 \cdot \log_{10} x_2}} = \frac{255}{1 + e^{-0.75 \cdot \log_{10}(Et_2)}} = \frac{255}{1 + e^{-0.75 \cdot \log_{10}(x_1 t_2/t_1)}}, \quad (10)$$

From Eq. (9),

$$x_1 = 10^{-4/3 \cdot \ln(\frac{255}{p_1} - 1)}, \quad (11)$$

with $p_1 \neq 0$ and $p_1 \neq 255$. According to Eq. (11), Eq. (10) can be expressed in the form:

$$p_2 = \frac{255}{1 + e^{-0.75 \cdot \log_{10}(10^{-4/3 \cdot \ln(\frac{255}{p_1} - 1)} \cdot t_2/t_1)}} = \frac{255}{1 + e^{\ln(\frac{255}{p_1} - 1) - \frac{3}{4} \log_{10}(t_2/t_1)}}. \quad (12)$$

By using Eq. (12), we could figure out the new pixel value when the camera exposure time is changed. On the other hand, when a pixel value is 0 or 255, it approaches a limit, either too dark or too bright. If p_1 approximates to 0, $\ln(255/p_1 - 1)$ is close to $+\infty$, the effect of exposure change is slight; if p_1 approximates to 255, $\ln(255/p_1 - 1)$ is close to $-\infty$, the effect of exposure change is also slight. So under these two conditions, we do not change the pixel value. If $p_1 = 0$, we assume $p_2 = 0$; if $p_1 = 255$, we assume $p_2 = 255$.

3.3 The Effect of Exposure Time Change

Scaling Factor (SF) is used to scale the quantization matrix recommended in the JPEG standard. The 'Lena' JPEG image with SF = 1 as shown in Fig. 1a is used in our experiments. The image size is 512-by-512 pixels. A 40-by-40 pixels binary logo called 'Fu' which is a Chinese character shown in Fig. 1b is used as a decodable watermark. The watermarked image through IWE and the corresponding decoded watermark are shown in Fig. 1c and Fig. 1d respectively. The exposure time of Fig. 1c is increased 1000 times. The resultant watermarked image and the corresponding decoded watermark are shown in Fig. 1e and Fig. 1f respectively. Then the exposure time of Fig. 1c is shortened 1000 times. The resultant watermarked image and the corresponding decoded watermark are shown in Fig. 1g and Fig. 1h respectively. Finally, Figs. 2 and 3 illustrate the influence of exposure time change of the watermarked image on normalized cross-correlation score s_1 and error rate during watermark decoding and detection. The error rate is used to refer to the percentage of incorrect pixels of the decoded watermark image. For any pixel of the decoded watermark image, if it is different from the pixel of the same location of the original watermark image, it is an incorrect pixel. Fig. 2 shows how s_1 drops and how error rate increases with the increase of the exposure time of the watermarked image. Fig. 3 shows how s_1 drops and how error rate increases with the decrease of the exposure time of the watermarked

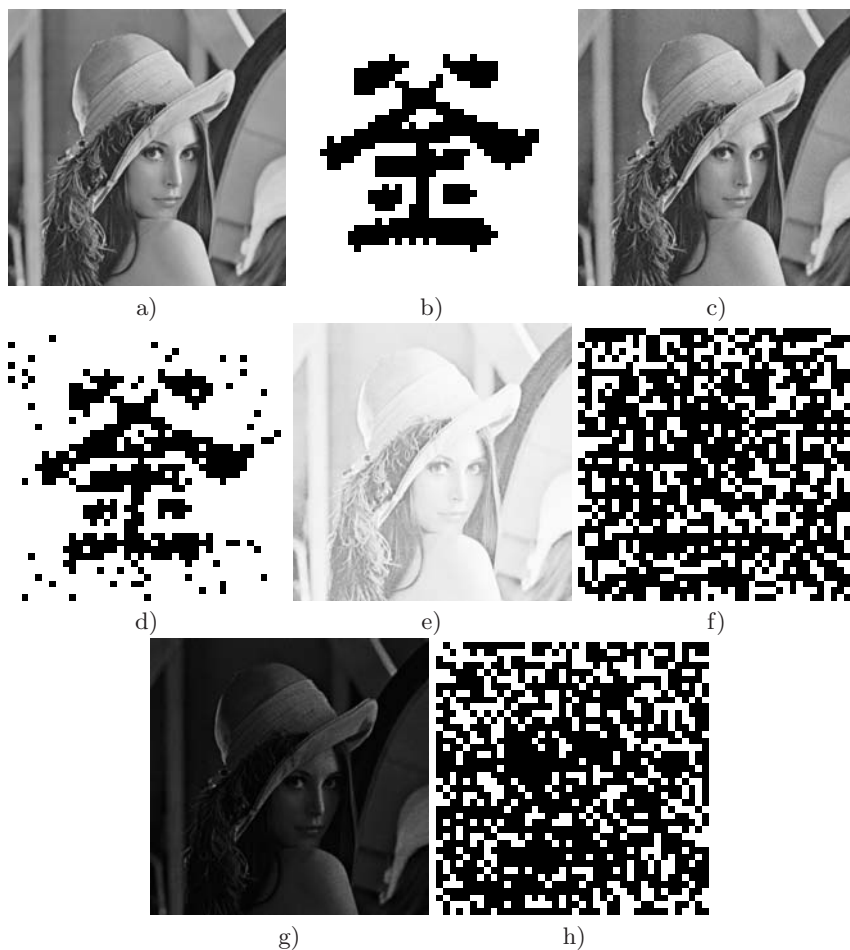


Fig. 1. ETC attack phase 1: a) Original host image; b) Original watermark; c) Watermarked image; d) Extracted watermark; e) Watermarked image with longer exposure time; f) Extracted watermark from e); g) Watermarked image with shorter exposure time; h) Extracted watermark from g)

image. As expected the larger extent of the exposure time change of the watermarked image, the harder for us to get the correct watermark during watermark decoding and detection.

3.4 Probability Analysis of the Results of Exposure Time Change

The aim of ETC attack is to decrease the cross-correlation score between the original watermark and the decoded watermark. It is expected that the

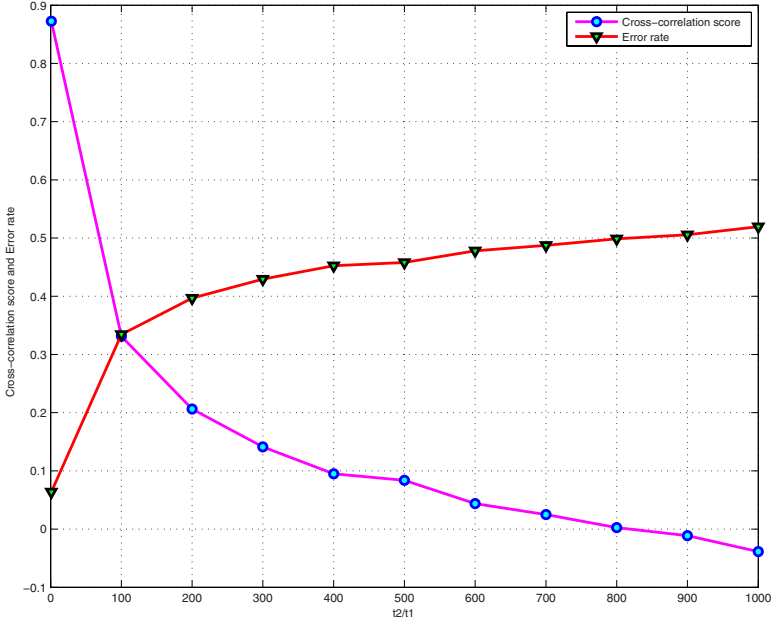


Fig. 2. The influence of longer exposure time on cross-correlation score s_1 and error rate

correlation between watermark decoded from the watermarked image and watermark decoded from the attacked image is weak. By probability term, we want

$$P\left(\text{OWM}(\vec{i}) = \text{ETCWM}(\vec{i})\right) = 0.5 \tag{13}$$

where OWM represents the watermark decoded from the watermarked image, ETCWM represents the watermark decoded from the attacked image, and \vec{i} denotes the coordinate of watermarks.

For $P\left(\text{OWM}(\vec{i}) = \text{ETCWM}(\vec{i})\right) = 1$, it is obvious that the ETC is of no effect to the watermark decoding. For $P\left(\text{OWM}(\vec{i}) = \text{ETCWM}(\vec{i})\right) = 0$, we derive the opposite image of OWM, where 1 corresponds to 0 in OWM and 0 corresponds to 1 in OWM. By reversing the opposite image, we could get OWM. When $P\left(\text{OWM}(\vec{i}) = \text{ETCWM}(\vec{i})\right) = 0.5$, the attack effect is best. Neither detectors or human eyes could find the watermark in that case.

4 ETC Phase 2: Image Fusion

Changing exposure time causes the disparity between the original image and differently-exposed images, which are either darker or brighter than original

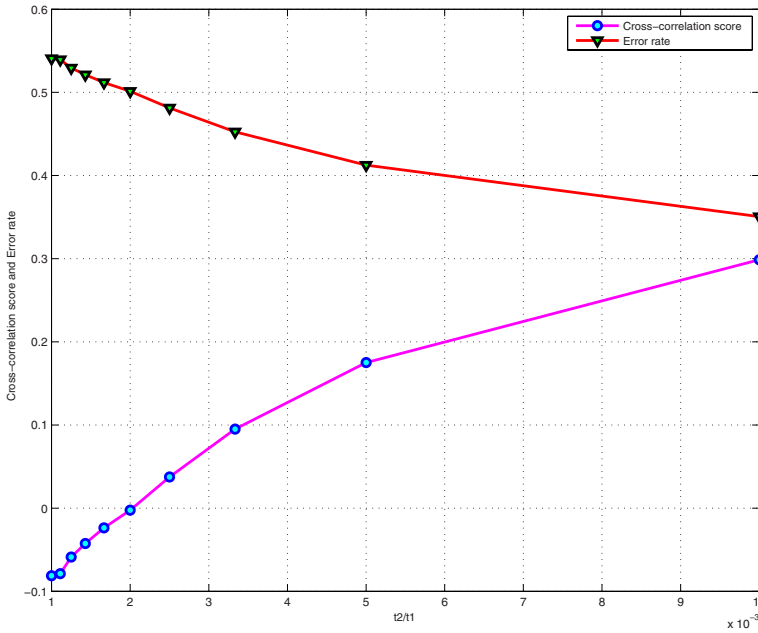


Fig. 3. The influence of shorter exposure time on cross-correlation score s_1 and error rate

image. In what follows, the disparity is larger as watermark detection becomes harder. The hope is that after a large exposure time is changed such that watermark detection becomes nearly impossible, the image after exposure time change can be turned to approximate to original image as closely as possible. We propose to use an image fusion method based on weighted average to combine differently-exposed images into a single composite image that is very similar to the original image for visual perception.

4.1 SSIM

We apply SSIM index [8] for measuring the disparity between the original image and differently-exposed images instead of PSNR or MSE because SSIM performs better with the qualitative visual appearance. When $SSIM = 1$, the disparity is non-existent. The two compared images look exactly the same. The smaller the SSIM index, the larger the disparity between the two compared images. The influence of exposure time change on SSIM index is shown in Fig. 4 and Fig. 5. Notably, the increase in exposure time change diminishes the similarity between the watermarked image and the original image. Note that the SSIM index between the original image and the watermarked image is 0.94. In comparison with Fig. 2 and Fig. 3, the problem now is how to keep balance between the similarity and the attack effect.

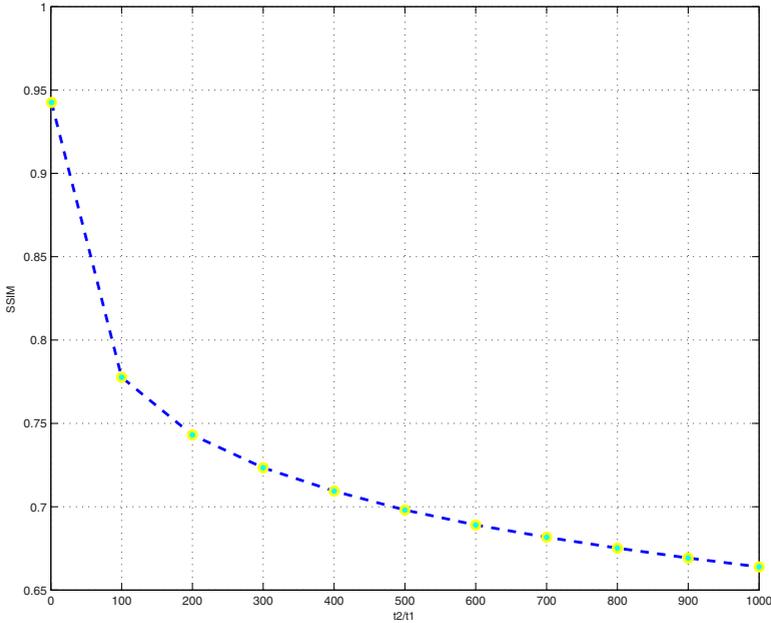


Fig. 4. The influence of longer exposure time on SSIM index

4.2 The Classification of Image Fusion Methods

Image fusion is the process of combining multiple images to offer an enhanced picture, which contains more desired features than input images. For a recent survey of image fusion research advances and challenges, the reader is referred to [9].

There are several types of image fusion methods. We distinguish between three main types based on their combination algorithms:

- *Average or weighted average method.* The resulting image pixel values are the arithmetic mean or the weighted average of corresponding pixel values of multiple images in the spatial domain. In general, it leads to a stabilization of the fusion result, whereas it introduces the problem of contrast reduction [10].
- *Image pyramids method* [11], [12]. A method first generates a sequence of image pyramids from each image. Then for each level, combination algorithm yields the composite image. At last, an inverse pyramid transform of the composite image is used to create the fused image.
- *Wavelet method* [13], [14]. A method similar to the image pyramids method. Instead, wavelet transform is used for the decomposition of the input images.

4.3 Fusion Algorithm

We have used three breeds of popular methods in image fusion mentioned above to combine differently-exposed images. Although the composite images constructed using the image pyramids method and the wavelet method are very

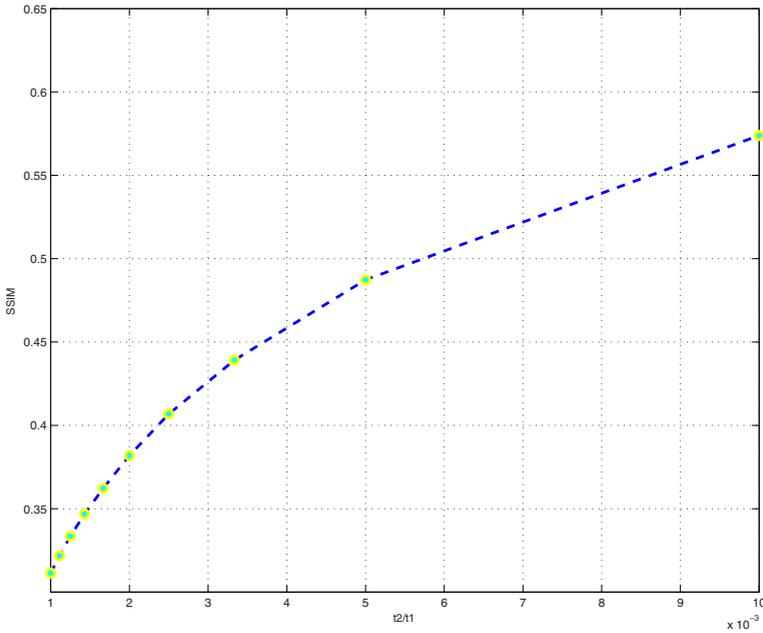


Fig. 5. The influence of shorter exposure time on SSIM index

similar to the original image, the attack effect is relatively poor when compared with the weighted average method. In addition, the image pyramids method and the wavelet method are more time-consuming than the weighted average method. Thus, We choose the weighted average approach to fuse images with different exposure time, which achieves better attack effect and is computationally efficient.

First we get a set of differently exposed images using method introduced in Sec. 3. Then each image is assigned to a weight. If there are k differently-exposed images (x_1, x_2, \dots, x_k) and their corresponding weights are $(\lambda_1, \lambda_2, \dots, \lambda_k)$, the fused image is

$$x^{wave} = \frac{\sum_{i=1}^k \lambda_i x_i}{\sum_{i=1}^k \lambda_i}. \quad (14)$$

According to Eq. (12), when we change exposure time of one image from t_1 to t_2 , for this change, the changed pixel value can be seen as a function of original pixel value. For the original image, the changed pixel value function F of original pixel value x is defined as

$$F(x) = \frac{255}{1 + e^{\ln(\frac{255}{x} - 1) - \frac{3}{4} \log_{10}(t_2/t_1)}}. \quad (15)$$

When we insert the watermark into the image to obtain the watermarked image either in the spatial domain or in the transform domain, we specify a parameter

ξ which determines the difference of one pixel's value between before and after the insertion. For the watermarked image, the changed pixel value function F of original pixel value $x + \xi$ can be defined as follows

$$F(x + \xi) = F(x) + \beta, \tag{16}$$

where β is the difference between one pixel's value of the original image after exposure time change and that of the watermarked image after exposure time change. By the mean value theorem we have

$$\beta = F(x + \xi) - F(x) = F'(x + \xi') \cdot \xi, \tag{17}$$

with $0 < \xi' < \xi$. We set

$$y(x) = e^{\ln(\frac{255}{x}) - 1} - \frac{3}{4} \log_{10}(t2/t1). \tag{18}$$

Using Eq. (18) we can write

$$\begin{aligned} F'(x) &= 255 \cdot \frac{-1}{(1+y)^2} \cdot \frac{dy}{dx}(x) \\ &= \frac{-255}{(1+y)^2} \cdot y \cdot \frac{1}{\frac{255}{x} - 1} \cdot \frac{-255}{x^2} \\ &= 255^2 \cdot \frac{y}{(1+y)^2} \cdot \frac{1}{(255-x) \cdot x}, \end{aligned} \tag{19}$$

hence

$$\beta = 255^2 \cdot \frac{e^{\ln(\frac{255}{x+\xi'}) - 1} - \frac{3}{4} \log_{10}(t2/t1)}{(1 + e^{\ln(\frac{255}{x+\xi'}) - 1} - \frac{3}{4} \log_{10}(t2/t1))^2} \cdot \frac{1}{(255 - x - \xi') \cdot (x + \xi')} \cdot \xi. \tag{20}$$

Using Eq. (14) and (16), the pixel value $x_{p,q}^{wave}$ of the resultant fused image in the position (p, q) can be calculated as follows

$$\begin{aligned} x_{p,q}^{wave} &= \frac{\sum_{i=1}^k \lambda_i F_{i,p,q}(x + \xi)}{\sum_{i=1}^k \lambda_i} \\ &= \frac{\sum_{i=1}^k \lambda_i (F_{i,p,q}(x) + \beta_{i,p,q})}{\sum_{i=1}^k \lambda_i} \\ &= \frac{\sum_{i=1}^k \lambda_i F_{i,p,q}(x)}{\sum_{i=1}^k \lambda_i} + \frac{\sum_{i=1}^k \lambda_i \beta_{i,p,q}}{\sum_{i=1}^k \lambda_i}, \end{aligned} \tag{21}$$

where $F_{i,p,q}(x + \xi)$ is the pixel value of the i -th watermarked image after exposure time change in the position (p, q) . Our purpose is that the resultant fused image is similar to the original image, while the watermark is nearly removed. The hope is to select the optimum weights to achieve our purposes. That is, after choosing optimum weight λ_i for each image to be fused, $\frac{\sum_{i=1}^k \lambda_i F_{i,p,q}(x)}{\sum_{i=1}^k \lambda_i}$ approaches to x

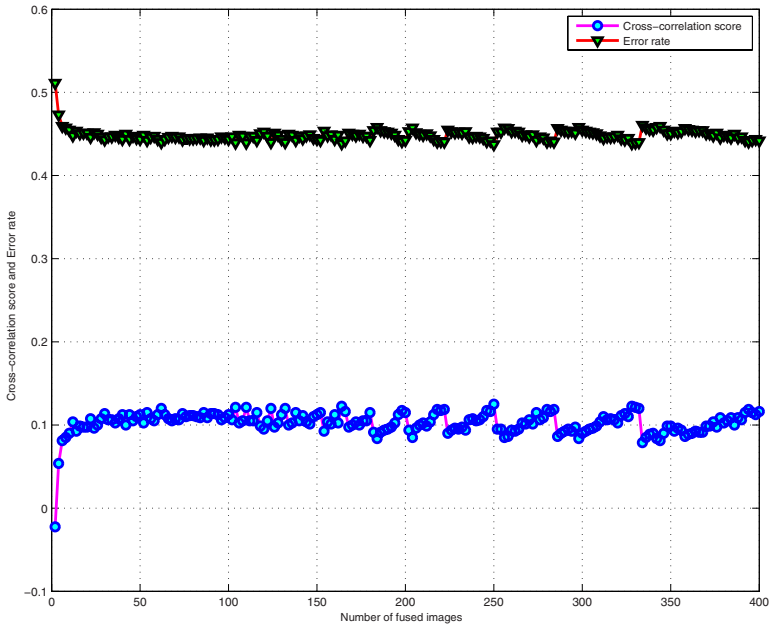


Fig. 6. The influence of the number of fused images on cross-correlation score s_1 and error rate

and $\frac{\sum_{i=1}^k \lambda_i \beta_{i,p,q}}{\sum_{i=1}^k \lambda_i}$ tends toward 0. We are currently investigating a method for selecting the optimum weights. In this paper, each image is assigned to a weight that depends on the extent of the exposure time change. The larger extent of the exposure time changes as compared to the watermarked image, the larger the weight.

4.4 Effect of Image Fusion

In our experiment, we choose images from a database of 2000 images with different exposure time as compared to the watermarked image. Fig. 6 illustrates how the cross-correlation score s_1 and error rate change as the number of fused image increases. Note that the error rates approximate to 0.5, which is a satisfactory result. The reasons can be seen in Sec. 3.4. Fig. 7 illustrates how the number of fused image influences the SSIM index. It can be observed that the attack effect of ETC phase 1 is preserved in the fusion process and the fused images are similar to the original image. The fused image from 400 images with different exposure time is shown in Fig. 8a. It can be seen that the fused image achieves good perceptual quality. Using the watermark decoding algorithm, we extract the watermark image from the fused image as shown in Fig. 8b. Clearly, the watermark cannot be successfully detected.

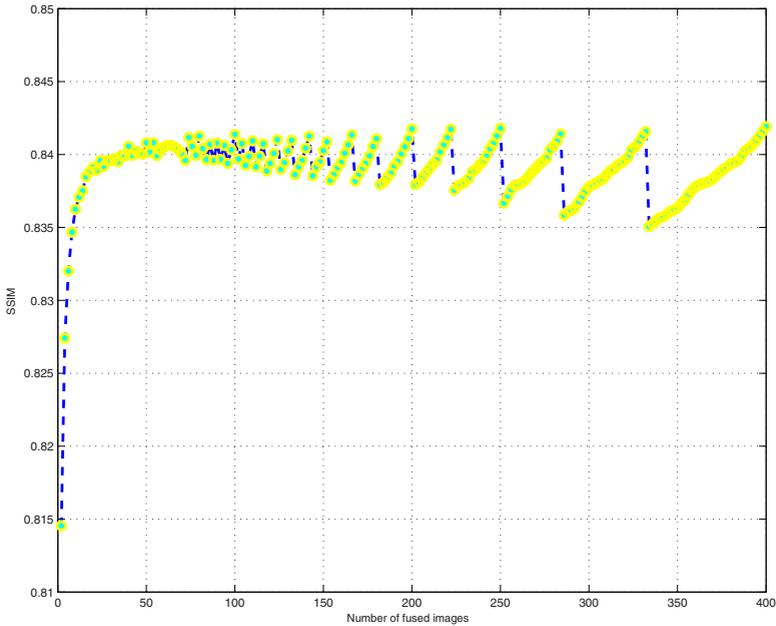


Fig. 7. The influence of the number of fused images on SSIM index



Fig. 8. ETC attack phase 2: a) Fused image; b) Decoded watermark from a).

5 Conclusion

In this paper, a new watermark attack paradigm ETC has been analyzed in detail. We find that many image watermarking systems can not derive the correct decoded watermark when the watermarked image is exposed differently. Both theoretical and experimental analyses have been given to support the proposed attack. The results show that our attack is successful with a reasonable image quality.

References

1. Kirovski, D., Petitcolas, F.: Blind pattern matching attack on watermarking systems. *IEEE Transactions on Signal Processing* 51, 1045–1053 (2003)
2. Maes, M.: Twin peaks: the histogram attack to fixed depth image watermarks. In: Aucsmith, D. (ed.) *IH 1998*. LNCS, vol. 1525, pp. 290–305. Springer, Heidelberg (1998)
3. Cox, I., Kilian, J., Leighton, F., Shamoon, T.: Secure spread spectrum watermarking for multimedia. *IEEE Transactions on Image Processing* 6, 1673–1687 (1997)
4. Xia, X., Boncelet, C., Arce, G.: A multiresolution watermark for digital images. In: *Proceedings of the International Conference on Image Processing*, vol. 1 (1997)
5. Wong, P.: Image watermarking and data hiding techniques. PhD thesis, Department of Electronic and Computer Engineering. The Hong Kong University of Science and Technology, Hong Kong, China (2003), <http://www.ece.ust.hk/~eepeter/paperpdf/Peter.PhD.Thesis.pdf>
6. Debevec, P., Malik, J.: Recovering high dynamic range radiance maps from photographs. In: *Proceedings of the 24th Annual Conference on Computer Graphics and Interactive Techniques*, pp. 369–378 (1997)
7. Bhukhanwala, S., Ramabadran, T.: Automated global enhancement of digitized photographs. *IEEE Transactions on Consumer Electronics* 40, 1–10 (1994)
8. Wang, Z., Bovik, A., Sheikh, H., Simoncelli, E.: Image quality assessment: from error visibility to structural similarity. *IEEE Transactions on Image Processing* 13, 600–612 (2004)
9. Ardeshir Goshtasby, A., Nikolov, S.: Image fusion: advances in the state of the art. *Information Fusion* 8, 114–118 (2007)
10. Piella, G.: A general framework for multiresolution image fusion: from pixels to regions. *Information Fusion* 4, 259–280 (2003)
11. Burt, P.: The pyramid as a structure for efficient computation. *Multiresolution Image Processing and Analysis* 35 (1984)
12. Sims, S., Phillips, M.: Target signature consistency of image data fusion alternatives. *Optical Engineering* 36, 743 (1997)
13. Zhang, Z., Blum, R.: A categorization of multiscale-decomposition-based image fusionschemes with a performance study for a digital camera application. *Proceedings of the IEEE* 87, 1315–1326 (1999)
14. Rockinger, O., Fechner, T.: Pixel-level image fusion: the case of image sequences. In: *Proceedings of the SPIE*, vol. 3374, pp. 378–388 (1998)